J|A|C|S ARTICLES

Published on Web 09/07/2010

Design, Synthesis, and Crystal Structures of 6-Alkylidene-2′-Substituted Penicillanic Acid Sulfones as Potent Inhibitors of *Acinetobacter baumannii* OXA-24 Carbapenemase

German Bou,[¶,†] Elena Santillana,[¶,‡] Anjaneyulu Sheri,[§] Alejandro Beceiro,[¶,†] Jared M. Sampson,[||] Matthew Kalp,[||] Christopher R. Bethel,[○] Anne M. Distler,[#] Sarah M. Drawz,[⊥] Sundar Ram Reddy Pagadala,[§] Focco van den Akker,[||] Robert A. Bonomo,[*,#,∇,○] Antonio Romero,[*,‡] and John D. Buynak[*,§]

Instituto de Investigación Biomédica de A Coruña (INIBIC), Complejo Hospitalario Universitario A Coruña, 15006-A Coruña, Spain, Centro de Investigaciones Biológicas, Consejo Superior de Investigaciones Cientificas (CIB-CSIC), E-28040 Madrid, Spain, Department of Chemistry, Southern Methodist University, Dallas, Texas 75275, Departments of Biochemistry, Pathology, and Pharmacology, Case Western Reserve University School of Medicine, and Department of Molecular Biology and Microbiology, Case Western Reserve University, Cleveland, Ohio 44106, and Infectious Diseases Section, Louis Stokes Cleveland Department of Veterans Affairs Medical Center, Cleveland, Ohio 44106

Received May 12, 2010; E-mail: jbuynak@smu.edu; romero@cib.csic.es; robert.bonomo@med.va.gov

Abstract: Class D β-lactamases represent a growing and diverse class of penicillin-inactivating enzymes that are usually resistant to commercial β-lactamase inhibitors. As many such enzymes are found in multidrug resistant (MDR) *Acinetobacter baumannii* and *Pseudomonas aeruginosa*, novel β-lactamase inhibitors are urgently needed. Five unique 6-alkylidene-2′-substituted penicillanic acid sulfones (**1**−**5**) were synthesized and tested against OXA-24, a clinically important β-lactamase that inactivates carbapenems and is found in *A. baumannii*. Based upon the roles Tyr112 and Met223 play in the OXA-24 β-lactamase, we also engineered two variants (Tyr112Ala and Tyr112Ala,Met223Ala) to test the hypothesis that the hydrophobic tunnel formed by these residues influences inhibitor recognition. IC_{50} values against OXA-24 and two OXA-24 β-lactamase variants ranged from 10 $\pm$ 1 (**4** vs WT) to 338 $\pm$ 20 nM (**5** vs Tyr112Ala, Met223Ala). Compound **4** possessed the lowest K_i (500 $\pm$ 80 nM vs WT), and **1** possessed the highest inactivation efficiency ($k_{inact}/K_i = 0.21 \pm 0.02\ \mu M^{-1}\ s^{-1}$). Electrospray ionization mass spectrometry revealed a single covalent adduct, suggesting the formation of an acyl-enzyme intermediate. X-ray structures of OXA-24 complexed to four inhibitors (2.0−2.6 Å) reveal the formation of stable bicyclic aromatic intermediates with their carbonyl oxygen in the oxyanion hole. These data provide the first structural evidence that 6-alkylidene-2′-substituted penicillin sulfones are effective mechanism-based inactivators of class D β-lactamases. Their unique chemistry makes them developmental candidates. Mechanisms for class D hydrolysis and inhibition are discussed, and a pathway for the evolution of the BlaR1 sensor of *Staphylococcus aureus* to the class D β-lactamases is proposed.

Introduction

β-Lactamase enzymes (EC 3.5.2.6) provide one of the most important mechanisms of resistance to β-lactam antibiotics in Gram-negative bacteria.[1−10] As the prevalence of resistant pathogens is increasing in health care institutions, this formidable

[¶] These authors contributed equally to this work.
[†] Universitario A Coruña.
[‡] CIB-CSIC.
[§] Department of Chemistry, Southern Methodist University.
[||] Department of Biochemistry, Case Western Reserve University School of Medicine.
[⊥] Department of Pathology, Case Western Reserve University School of Medicine.
[#] Department of Pharmacology, Case Western Reserve University School of Medicine.
[∇] Department of Molecular Biology and Microbiology, Case Western Reserve University.
[○] Louis Stokes Cleveland Department of Veterans Affairs Medical Center.

(1) Bush, K. *Clin. Microbiol. Infect.* **2008**, *14* (Suppl. 1), 134.
(2) Bush, K.; Jacoby, G. A. *Antimicrob. Agents Chemother.* **2010**, *54*, 969.
(3) Bush, K.; Mobashery, S. *Adv. Exp. Med. Biol.* **1998**, *456*, 71.
(4) Fisher, J. F.; Meroueh, S. O.; Mobashery, S. *Chem. Rev.* **2005**, *105*, 395.
(5) Frère, J. M.; Dubus, A.; Galleni, M.; Matagne, A.; Amicosante, G. *Biochem. Soc. Trans.* **1999**, *27*, 58.
(6) Kotra, L. P.; Mobashery, S. *Arch. Immunol. Ther. Exp. (Warsz.)* **1999**, *47*, 211.
(7) Livermore, D. M. *Curr. Protein Pept. Sci.* **2009**, *10*, 397.
(8) Matagne, A.; Dubus, A.; Galleni, M.; Frère, J. M. *Nat. Prod. Rep.* **1999**, *16*, 1.
(9) Philippon, A.; Dusart, J.; Joris, B.; Frere, J. M. *Cell. Mol. Life Sci.* **1998**, *54*, 341.
(10) Queenan, A. M.; Bush, K. *Clin. Microbiol. Rev.* **2007**, *20*, 440.

 10.1021/ja104092z

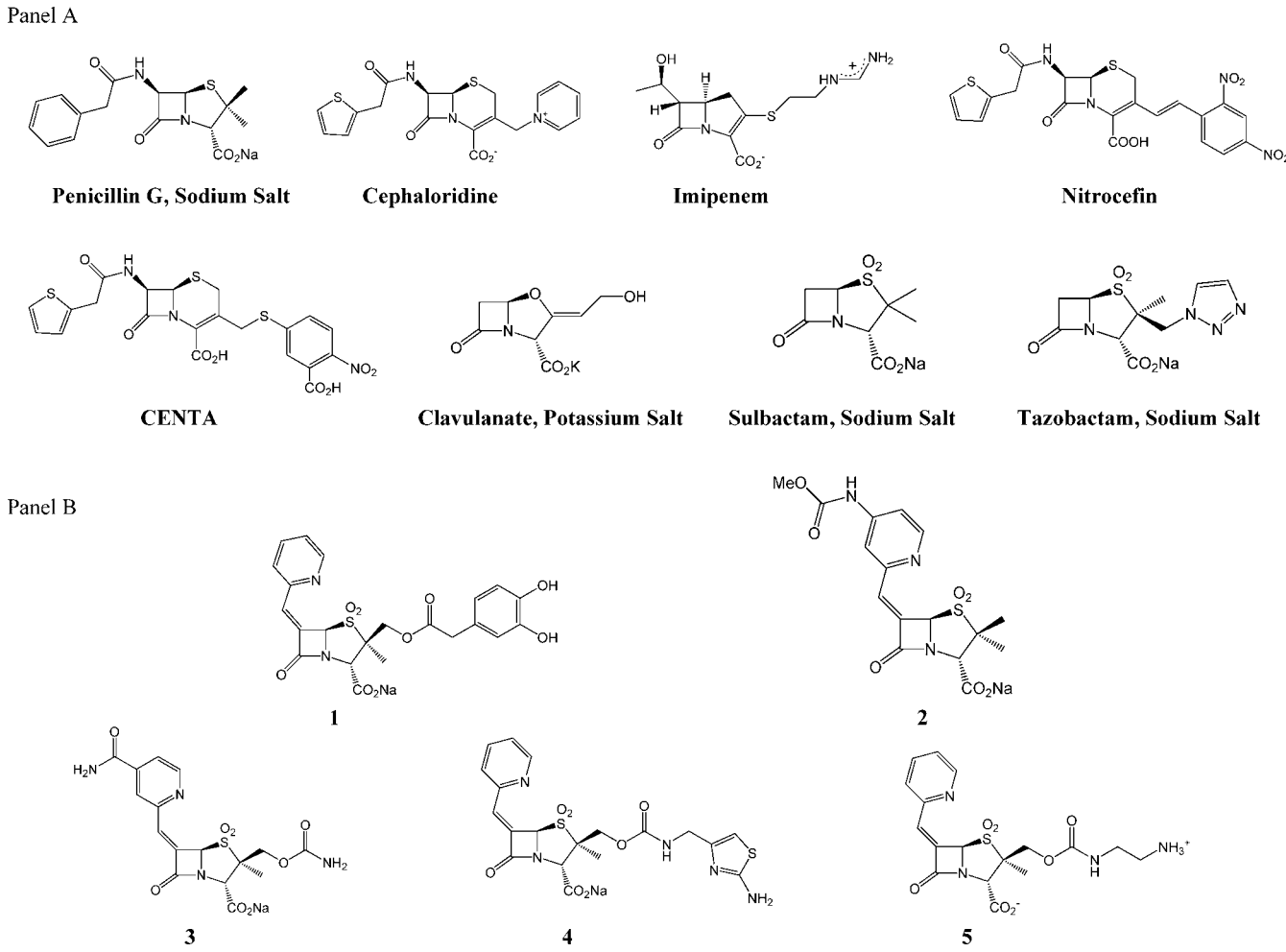

Figure 1. Chemical structures of substrates, commercially available inhibitors (sulbactam, tazobactam, and clavulanic acid), and 6-alkylidene-2′-substituted penicillanic acid sulfone compounds used in this study. The chemical structure of penicillin G is presented as a model for all penicillins. In like manner, cephaloridine and imipenem are presented as models for cephalosporins and carbapenems.

challenge is creating significant concern among the medical and scientific community.[2,11] Currently, there are more than 870 unique, naturally occurring β-lactamases.[2] Based on protein sequence similarities, four major β-lactamase classes are described (classes A−D).[12−15] The class A, C, and D enzymes use serine as the active-site, reactive nucleophile. Class B enzymes are metallo-β-lactamases that use one or two Zn^{2+} atoms to catalyze the hydrolysis of the β-lactam bond.[4] In general, serine β-lactamases inactivate β-lactams by a two-step reaction mechanism:

$$E + S \underset{k_{-1}}{\overset{k_1}{\rightleftharpoons}} E{:}S \xrightarrow{k_2} E{-}S \xrightarrow[H_2O]{k_3} E + P \qquad (1)$$

Here, E represents the β-lactamase, S is the β-lactam substrate, E:S is the Henri−Michaelis complex, E−S is the acyl-enzyme, and P is the inactive product.

The most rapidly growing and diverse group of β-lactamases are the class D enzymes.[16] As a group, class D β-lactamases, also called "oxacillinases", hydrolyze penicillins, cephalosporins, and carbapenems (Figure 1, Panel A). Unlike class A enzymes, class D β-lactamases are typically resistant to inhibition by clavulanate, sulbactam, and tazobactam. In order to preserve the current β-lactam antibiotics, potent inhibitors of class D oxacillinases are urgently needed.[17,18]

Among the many experimental β-lactamase inhibitors that were developed, Chen et al. designed the 6*Z*-(α-pyridylmethylidene) penicillin sulfone series and showed them to be potent compounds with the ability to inactivate a wide spectrum of serine β-lactamases.[19] Buynak et al. later demonstrated that the incorporation of a 2′ substitution (Figure 1B, compound **1**) could both improve synergy and augment the inhibitory spectrum of this series.[20−25] Based upon a consideration of the potency of

(11) Rice, L. B. *Curr. Opin. Microbiol.* **2009**, *12*, 476.
(12) Ambler, R. P. *Philos. Trans. R. Soc. London B Biol. Sci.* **1980**, *289*, 321.
(13) Ambler, R. P.; Coulson, A. F.; Frère, J. M.; Ghuysen, J. M.; Joris, B.; Forsman, M.; Levesque, R. C.; Tiraby, G.; Waley, S. G. *Biochem. J.* **1991**, *276* (Pt. 1), 269.
(14) Jaurin, B.; Grundstrom, T. *Proc. Natl. Acad. Sci. U.S.A.* **1981**, *78*, 4897.
(15) Ouellette, M.; Bissonnette, L.; Roy, P. H. *Proc. Natl. Acad. Sci. U.S.A.* **1987**, *84*, 7378.
(16) Poirel, L.; Naas, T.; Nordmann, P. *Antimicrob. Agents Chemother.* **2010**, *54*, 24.
(17) Drawz, S. M.; Bonomo, R. A. *Clin. Microbiol. Rev.* **2010**, *23*, 160.
(18) Perez-Llarena, F. J.; Bou, G. *Curr. Med. Chem.* **2009**, *16*, 3740.
(19) Chen, Y. L.; Chang, C. W.; Hedberg, K. *Tetrahedron Lett.* **1986**, *27*, 3449.
(20) Buynak, J. D. *Curr. Med. Chem.* **2004**, *11*, 1951.
(21) Buynak, J. D. *Biochem. Pharmacol.* **2006**, *71*, 930.
(22) Buynak, J. D.; Chen, H.; Vogeti, L.; Gadhachanda, V. R.; Buchanan, C. A.; Palzkill, T.; Shaw, R. W.; Spencer, J.; Walsh, T. R. *Bioorg. Med. Chem. Lett.* **2004**, *14*, 1299.

Scheme 1. Model for Inhibition Proposed on the Basis of Analyses of the C2/3-Substituted Penicillin and Cephalosporin Sulfone Series against OXA β-Lactamases[28] [a]

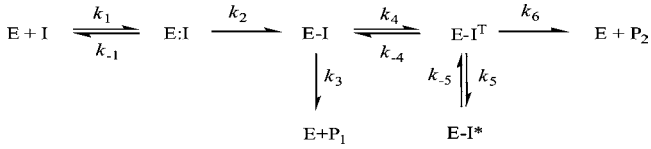

[a] In this model, E:I represents the formation of the pre-acylation complex and E-I, the acyl-enzyme species. The acyl-enzyme (E-I) can proceed to hydrolysis (E + P_1) or undergo rearrangement to a transiently inhibited species (E-I^T). The E-I^T intermediate may then return to E-I, proceed to hydrolysis (E + P_2), or form an inactivated acyl-enzyme (E-I*). The rate constants, *k*, describing each of these steps are also represented.

1 and related compounds against class A β-lactamases compared to clavulanate, sulbactam, and tazobactam, a reaction mechanism was hypothesized.

To elucidate this mechanism, an analysis of SHV-1 inactivated by **1** was undertaken.[26] A complex of **1** with SHV-1 (PDB 3D4F) showed that the inhibitor's C6 (heteroaryl)alkylidene group plays a critical role in the formation of a planar bicyclic aromatic intermediate. Moreover, the pyridyl nitrogen of the C6 substituent nucleophilically adds to the intermediate imine, leading to the formation of a bicyclic aromatic species (indolizine). Furthermore, the crystal structure showed that the acyl-enzyme ester carbonyl of the intermediate is resonance stabilized by the conjugated π system and the carbonyl group of the intermediate is positioned outside the oxyanion hole. The decreased deacylation rates of this species are likely due to resonance stabilization, the location of the carbonyl at an increased distance from the hydrolytic water, and improper positioning for nucleophilic attack by the enzyme's backbone nitrogens.

A recent investigation involving the synthesis and microbiological evaluation of more than 100 substituted analogues of the general 6-(pyridylmethylidene)penam sulfone inhibitory subtype revealed that many of these derivatives, particularly those incorporating 2′ substitutions, were also potent submicromolar inhibitors of the class D OXA-24 carbapenemase.[27] In addition, many showed synergy with carbapenems against resistant microorganisms. These findings are especially noteworthy as the commercially available inhibitors are ineffective against class D β-lactamases. A comparative susceptibility and kinetic study of OXA-1, -10, -14, -17, and -24 β-lactamases with **1** and related compounds established the potential efficacy of these inhibitors. This analysis was consistent with a branched pathway model for inhibition (Scheme 1 and ref 28) and served as a springboard for more in-depth analyses.

Here we present the design, synthesis, and characterization of novel potent 6*Z*-(α-pyridylmethylidene)penam sulfone inhibitors against OXA-24 β-lactamase. Inhibitors **1**, **2**, **3**, and **5** were complexed with OXA-24 (also known as OXA-40). A previous report by Santillana et al. showed that carbapenem substrate specificity is largely determined by a hydrophobic barrier that is established through an arrangement of the Tyr112 and Met223 side chains.[29] Tyr112 and Met223 residues define a tunnel-like entrance to the active site. To test the contribution of these important residues to the inhibitor profile, the Tyr112Ala and Tyr112Ala/Met223Ala β-lactamases were also assayed in inhibition studies. We show for the first time that 6-alkylidene-2′-substituted penicillin sulfone inhibitors are effective mechanism-based inactivators for this challenging class of β-lactamases; their unique reaction chemistry makes them suitable lead compounds for further development.

Materials and Methods

Chemical Syntheses. The design, synthesis, and evaluation of **1** were previously reported.[25,26] Compounds **2**−**5** were synthesized as part of a drug discovery effort.[27] The chemical structures of the compounds studied are illustrated in Figure 1, Panel B, and details of each synthesis are presented in Supporting Information (SI) Schemes 1−3 and discussed below.

Genetic Constructs and Host Strains. $bla_{\text{OXA-24}}$ (also named $bla_{\text{OXA-40}}$) was isolated from a strain of *Acinetobacter baumannii* RYC 52763/97.[30] The wild-type (WT) $bla_{\text{OXA-24}}$ and mutated genes were subcloned into pGEX-6p-1 (*Bam*HI and *Eco*RI restriction sites) to generate a fusion protein between GST and the OXA-24 lacking the signal peptide.

$bla_{\text{OXA-24}}$ and the mutated $bla_{\text{OXA-24}}$ genes ($bla_{\text{OXA-24-Tyr112Ala}}$, $bla_{\text{OXA-24-Met223Ala}}$, and $bla_{\text{OXA-24-Tyr112Ala, Met223Ala}}$) were directionally subcloned into the pAT-RA plasmid (rifampin resistance) at the *Sma*I and *Eco*RI restriction sites under the control of the $bla_{\text{CTX-M-14}}$ β-lactamase gene promoter. Once the correct constructs were confirmed by DNA sequencing, the different plasmids were electroporated into the carbapenem-susceptible clinical strain, *A. baumannii* JC7/04.[29]

Antibiotic Susceptibility. Antibiotic susceptibility profiles were determined in cation-adjusted Mueller−Hinton broth by microdilution testing following Clinical Laboratory Standards Institute (CLSI) criteria.[31] Five different inhibitor compounds, **1**−**5**, were tested for their capacity to inhibit *A. baumannii* strain JC7/04 that possessed the different $bla_{\text{OXA-24}}$ genes. The inhibitors were tested at two concentrations, 4 and 16 μg/mL, in the presence of either imipenem (Merck) or meropenem (AstraZeneca). As a comparator inhibitor, tazobactam was used (Wyeth) at two different concentrations, 4 and 16 μg/mL. Minimal inhibitory concentrations (MICs) were determined in the presence of 50 μg/mL rifampin (Sigma). The MICs reported are the results of three independent experiments.

Kinetic Parameters. The half-maximum inhibitory concentrations (IC_{50}s) were determined using two different approaches. In a first set of experiments, we used 3-[(3-carboxy-4-nitrophenyl)sulfanylmethyl]-8-oxo-7-[(2-thiophen-2-ylacetyl)amino]-5-thia-1-azabicyclo[4.2.0]oct-2-ene-2-carboxylic acid (CENTA, Figure 1A) (Calbiochem EMD, San Diego, CA) at 25 μM as an indicator substrate.[32] We incubated the different inhibitors and β-lactamases for 10 min (complete inactivation) at 37 °C before measuring the remaining enzymatic activity.[32] The β-lactamases were used in the reactions at 0.13, 0.12, and 0.072 nM concentrations for OXA-24

(23) Buynak, J. D.; Doppalapudi, V. R.; Adam, G. *Bioorg. Med. Chem. Lett.* **2000**, *10*, 853.
(24) Buynak, J. D.; Doppalapudi, V. R.; Rao, A. S.; Nidamarthy, S. D.; Adam, G. *Bioorg. Med. Chem. Lett.* **2000**, *10*, 847.
(25) Buynak, J. D.; Rao, A. S.; Doppalapudi, V. R.; Adam, G.; Petersen, P. J.; Nidamarthy, S. D. *Bioorg. Med. Chem. Lett.* **1999**, *9*, 1997.
(26) Pattanaik, P.; Bethel, C. R.; Hujer, A. M.; Hujer, K. M.; Distler, A. M.; Taracila, M.; Anderson, V. E.; Fritsche, T. R.; Jones, R. N.; Pagadala, S. R.; van den Akker, F.; Buynak, J. D.; Bonomo, R. A. *J. Biol. Chem.* **2009**, *284*, 945.
(27) Sheri, A.; Pagadala, S. R. R.; Young, K.; Barrett, J. F.; Raghoobar, S. L.; Hairston, N. N.; Wisniewski, D.; Ogawa, A.; Motyl, M.; Hermes, J.; Park, Y. W.; Buynak, J. D. Presented at the *49th Intersci. Conf. Antimicrob. Agents Chemother.*, 2009, Poster F1-1496.
(28) Drawz, S. M.; Bethel, C. R.; Doppalapudi, V. R.; Sheri, A.; Pagadala, S. R.; Hujer, A. M.; Skalweit, M. J.; Anderson, V. E.; Chen, S. G.; Buynak, J. D.; Bonomo, R. A. *Antimicrob. Agents Chemother.* **2010**, *54*, 1414.
(29) Santillana, E.; Beceiro, A.; Bou, G.; Romero, A. *Proc. Natl. Acad. Sci. U.S.A.* **2007**, *104*, 5354.
(30) Bou, G.; Oliver, A.; Martinez-Beltran, J. *Antimicrob. Agents Chemother.* **2000**, *44*, 1556.
(31) CLSI. 2003.
(32) Sirot, D.; Recule, C.; Chaibi, E. B.; Bret, L.; Croize, J.; Chanal-Claris, C.; Labia, R.; Sirot, J. *Antimicrob. Agents Chemother.* **1997**, *41*, 1322.

WT, the OXA-24 doubly substituted enzyme, and OXA-24 Tyr112Ala, respectively. These determinations were performed at 25 °C in a Nicolete Evolution 300 spectrophotometer (Thermo Electron Corp., Waltham, MA) with quartz cuvettes of 1 cm optical path length (each determination was done in triplicate).

We also used nitrocefin (NCF, Figure 1A) (100 μM) as the indicator substrate, incubating the enzymes and inhibitors at room temperature using 3.5 nM OXA-24 and 7 nM of each variant. Residual velocities were determined after 10 min. The data were plotted as 1/velocity ($1/v$) as a function of inhibitor concentration (I) and fitted to a linear equation, and the value of IC_{50} was determined by dividing the y-intercept by the slope of the line.

Steady-state kinetic parameters were determined using an Agilent 8453 diode array spectrophotometer.[33] The kinetic determinations were performed at room temperature in 50 mM sodium phosphate supplemented with a saturating concentration of sodium bicarbonate (20 mM).[34] First, the kinetic parameters, V_{max} and K_m, were obtained with non-linear least-squares fits of the data (Henri−Michaelis equation) using Enzfitter (Biosoft Corp., Ferguson, MO):

$$v = V_{max}[S]/(K_m + [S]) \quad (2)$$

We determined the K_i for the inhibitors by measuring initial steady-state velocities in the presence of a constant concentration of enzyme (E, 7 nM) with increasing concentrations of inhibitor against 100 μM of the indicator substrate NCF. The competition assay between the inhibitor, I, and substrate, S, in the reaction can be represented by Scheme 1. Assuming this competitive mode of inhibition, initial velocity (v_0) measurements immediately after mixing yield a K_i which closely approximates K_m, as represented by the following equation:

$$v_0 = (V_{max}[S])/(K_m(1 + [I]/K_i) + [S]) \quad (3)$$

The data were plotted as $1/v$ as a function of inhibitor concentration, fitted to a linear equation, and the value of K_i determined by dividing the y-intercept by the slope of the line. The K_i (observed) value was corrected to account for the affinity of NCF for the OXA β-lactamases.[35]

$$K_i(\text{corrected}) = K_i(\text{observed})/[1 + ([S]/K_{mNCF})] \quad (4)$$

The first-order rate constant for enzyme and inhibitor complex inactivation, k_{inact}, was measured directly by monitoring the reaction time courses in the presence of inhibitors (I) **1**−**5**. Fixed concentrations of enzyme (E, 7 nM) and NCF and increasing concentrations of I were used in each assay. The k_{obs} values were determined using a non-linear least-squares fit of the data to eq 5 using Origin 7.5:

$$A = A_0 + v_f t + (v_0 - v_f)[1 - \exp(-k_{obs}t)]/k_{obs} \quad (5)$$

Here, A is absorbance, v_0 (expressed in variation of absorbance per unit time) is initial velocity, v_f is final velocity, and t is time. Each k_{obs} was plotted versus I and fit to determine k_{inact}.[33,34]

Electrospray Ionization Mass Spectrometry (ESI-MS). ESI-MS of the intact OXA β-lactamases inactivated by **1**, **3**, **4**, and **5** was performed on an Applied Biosystems (Framingham, MA) Q-STAR XL quadrupole time-of-flight mass spectrometer equipped with a nanospray source as described previously.[33,34] Experiments were conducted by first desalting the reaction mixtures using C_{18} ZipTips (Millipore, Bedford, MA) according to the manufacturer's protocol. The protein sample was then diluted with 50% acetonitrile/0.1% trifluoroacetic acid to a concentration of 10 μM. This protein solution was then infused into the mass spectrometer at a rate of 0.5 μL/min, and data were collected for 2 min. Spectra were deconvoluted using the Applied Biosystems Analyst program.

Protein Purification and Crystallization. The recombinant β-lactamase was then purified to homogeneity using the GST Gene Fusion System (Amersham Pharmacia Biotech, Europe GmbH). The mature purified β-lactamases lacking the GST fusion protein appeared on sodium dodecyl sulfate−polyacrylamide gels as a band of approximately 29 kDa (≥95% purity). From purified OXA-24 β-lactamase, tetragonal crystals were grown by the hanging drop vapor diffusion method in a crystallization solution containing 0.1 M sodium acetate and 28% PEG 2000 MME buffered with 0.1 M HEPES (pH 7.5). Diffraction-quality crystals were obtained by mixing equal volumes of the crystallization solution with protein at a concentration of 6 mg/mL. Bipyramidal-shaped crystals grew in a period of 5−8 days, reaching their maximal dimensions of $0.15 \times 0.15 \times 0.10$ mm^3. The crystals belong to space group $P4_12_12$, with one molecule in the asymmetric unit (Table 1). The first trials to co-crystallize the β-lactamase in complex with several of the selected inhibitors were unsuccessful. The crystals with the inhibitor were poorly defined in the electron density maps. To solve this, crystals were subjected to different soaking times while varying the concentration of the inhibitor. This was intended to stabilize the crystals and minimize cracking. Final optimized conditions were determined at incubation times as short as 5 min as the crystallization conditions containing also 3 mM of the corresponding inhibitor. Furthermore, **3** was incubated with the enzyme for 15 min at 10 mM concentration to test time-dependent inhibition (**3b**).

Data Collection, Structure Determination, and Refinement. Crystals were transferred into a crystallization solution containing 15% (v/v) PEG 400 for cryoprotection before immersion into liquid N_2 for data collection. X-ray diffraction data for **1**, **2**, **3**, and **5** inhibitor complexes were collected at the European Synchrotron Radiation Facility (ESRF, Grenoble, France) beamlines ID14-EH1, ID14-EH2, and ID14-EH4 using single frozen crystals (100 K). Inhibitor **3b** data were collected at beamline X-29 at the National Synchrotron Light Source (Brookhaven National Laboratory, Upton, NY). Diffraction images were indexed and integrated with MOSFLM.[36] Data for the **3b** complex were processed using HKL2000.[37] Data scaling, merging, and reduction were carried out with programs of the CCP4 suite.[38] Relevant statistics are presented in Table 1.

The structure of native OXA-24, crystallized at pH 7.5, was determined by difference Fourier techniques using the protein atomic coordinates of the original OXA-24 β-lactamase crystallized at pH 4.5 (PDB entry 2JC7).[29] Carbamylation of Lys84 was clearly visible in the electron density maps and could be built with confidence using COOT.[39] Moreover, this new crystal form shows the absence of the sulfate ion in the active site of the enzyme, making it a better target that could help address the structural studies of the selected inhibitors.

The model was subjected to several rounds of refinement with the program REFMAC,[40] whereas interactive model building used COOT.[39] Water molecules were modeled according to residual density profiles and geometrical requirements for hydrogen bonding. The crystallographic R-factor of the model is 19.7% for all unique reflections from 8.0 to 1.97 Å resolution (R_{free} = 24.4%).

The structures of OXA-24 in complex with four different penicillin sulfone-based inhibitors were solved by Fourier synthesis

(33) Bethel, C. R.; Distler, A. M.; Ruszczycky, M. W.; Carey, M. P.; Carey, P. R.; Hujer, A. M.; Taracila, M.; Helfand, M. S.; Thomson, J. M.; Kalp, M.; Anderson, V. E.; Leonard, D. A.; Hujer, K. M.; Abe, T.; Venkatesan, A. M.; Mansour, T. S.; Bonomo, R. A. *Antimicrob. Agents Chemother.* **2008**, *52*, 3135.
(34) Papp-Wallace, K. M.; Bethel, C. R.; Distler, A. M.; Kasuboski, C.; Taracila, M.; Bonomo, R. A. *Antimicrob. Agents Chemother.* **2010**, *54*, 890.
(35) De Meester, F.; Joris, B.; Reckinger, G.; Bellefroid-Bourguignon, C.; Frère, J. M.; Waley, S. G. *Biochem. Pharmacol.* **1987**, *36*, 2393.
(36) Leslie, A. G. *Acta Crystallogr. D Biol. Crystallogr.* **2006**, *62*, 48.
(37) Kabsch, W. *J. Appl. Crystallogr.* **1993**, *26*, 795.
(38) *Acta Crystallogr. D Biol. Crystallogr* **1994**, *50*, 760.
(39) Emsley, P.; Cowtan, K. *Acta Crystallogr. D Biol. Crystallogr.* **2004**, *60*, 2126.
(40) Murshudov, G. N.; Vagin, A. A.; Dodson, E. J. *Acta Crystallogr. D Biol. Crystallogr.* **1997**, *53*, 240.

Table 1. Data Collection and Refinement Statistics

	native	2	3	3b	5
			Data Collection		
space group	$P4_12_12$	$P4_12_12$	$P4_12_12$	$P4_12_12$	$P4_12_12$
cell dimensions [*a*, *b*, *c* (Å)]	102.4, 102.4, 84.1	102.4, 102.4, 84.2	102.8, 102.8, 83.1	103.1, 103.1, 85.8	102.5, 102.5, 84.5
resolution (Å)[a]	45.8−1.9 (2.0−1.9)	45.8−2.0 (2.11−2.0)	72.7−2.10 (2.21−2.10)	32.6−2.60 (2.67−2.6)	45.8−2.0 (2.11−2.0)
R_{merge} (%)	7.3 (67.7)	7.6 (54.0)	10.1 (62.1)	11.0 (30.1)	7.8 (56.4)
$I/\sigma(I)$	9.6 (1.1)	9.0 (1.4)	6.8 (1.1)	12.1 (2.1)	9.2 (1.4)
completeness (%)	100 (100)	99.9 (99.8)	99.0 (99.0)	93.4 (59.2)	99.9 (99.1)
redundancy	9.6 (9.5)	9.6 (9.8)	7.3 (4.4)	6.0 (2.1)	9.5 (9.5)
			Refinement		
resolution (Å)	45.8−1.97	45.8−2.0	54.7−2.10	32.6−2.60	45.8−2.0
no. of reflections	30 384	30 828	26 265	13 058	30 940
R_{work} /R_{free} (%)	19.7/24.4	22.2/25.7	23.2/25.5	17.4/21.1	22.1/24.8
no. of atoms					
protein	1939	1939	1939	1958	1939
ligand	0	27	29	29	29
PEG (SO_4)	0	0	13	4	13
solvent	158	112	79	105	116
B-factors					
protein	33.1	34.9	33.5	27.2	33.3
ligand	0	67.5	49.6	55.8	65.9
PEG/SO_4	0	0	46.7	81.1	60.0
solvent	40.1	39.4	37.3	28.3	40.0
rms deviations					
bond lengths (Å)	0.006	0.008	0.007	0.011	0.009
bond angles (°)	1.2	1.3	1.2	1.39	1.5
PDB code	3G4P	3FV7	3FYZ	3MBZ	3FZC

[a] Highest resolution shell is shown in parentheses.

employing the coordinates of the native enzyme. Refinement of these structures was carried out with CNS[41] and REFMAC.[40] After rigid-body refinement and model fitting, the position of the inhibitors was clearly defined in the active binding site, covalently attached to the active serine Ser81, from the electron density maps. Topology and parameter values for each of the ligands, **1**, **2**, **3**, and **5**, were generated using the Dundee PRODRG2 server.[42] Several rounds of refinement were combined with model rebuilding in COOT after inspection of electron density maps. All residues are in the most-favored and additionally allowed regions of the Ramachandran plot. A summary of refinement statistics is presented in Table 1. Structural figures were drawn using Chimera[43] or Pymol.[44] Electrostatic potential surfaces were calculated with GRASP.[45]

Results and Discussion

Inhibitor Design and Chemical Syntheses. With the knowledge of the mechanism of inhibition depicted in Scheme 1 and previous results regarding structure−activity relationships (SARs) due to modification of the 2′β position,[25] we synthesized compounds **1**−**5** according to the following plan.

As shown in SI Scheme 1, the carboxylic acid and amino functionalities of the commercially available 6-aminopenicillanic acid (6-APA) were sequentially protected by treatment with diphenyldiazomethane and allyl chloroformate, respectively, and the sulfur was oxidized to the corresponding sulfoxide with *m*CPBA. Utilizing the method of Kamiya,[46] the protected penam sulfoxide **6** was heated in the presence of mercaptobenzothiazole to generate an intermediate sulfenic acid, which was trapped *in situ* to generate the disulfide **7**. The thiazolidine was regenerated by treatment with silver acetate in the presence of chloroacetic acid to stereoselectively produce the 2′β-functionalized penam **8**, together with the cepham **9**. After the C6 and C7 amines were deprotected, this mixture was converted to the corresponding diazo compounds and treated with a catalytic amount of rhodium octanoate in the presence of excess propylene oxide to generate the corresponding 6-oxopenicillinates and 7-oxocephalosporinates (**12** and **13**), respectively.[47] Reaction with α-pyridylmethylenetriphenylphosphorane selectively produced the olefins of the *Z*-geometry. Separation of the penam and cephem isomers was achieved by oxidation of the mixture with *m*CPBA, which quickly oxidizes the cephalosporin to the sulfone **17** while leaving most of the more hindered sulfur of the penicillin at the sulfoxide oxidation state in **16**. Subsequent oxidation of the penicillin sulfoxide **16** to the corresponding sulfone, removal of the chloroacetate protecting group, and activation of the 2′β alcohol as the *p*-nitrophenyl carbonate produced intermediate **20**. Intermediate **20** was then reacted with the appropriate amine and the benzhydryl ester removed to produce the inhibitors **4** (compound **22**) and **5** (compound **24**).

As shown in SI Scheme 2, the functionalized pyridyl moiety was prepared from commercially available 2,4-lutidine, which undergoes selective oxidation of the C4 methyl group upon treatment with potassium permanganate.[48] Generation of the corresponding acid chloride and reaction with allyl alcohol produced ester **26**, which was converted to the corresponding pyridine *N*-oxide **27** upon treatment with *m*CPBA. Treatment

(41) Brunger, A. T.; Adams, P. D.; Clore, G. M.; DeLano, W. L.; Gros, P.; Grosse-Kunstleve, R. W.; Jiang, J. S.; Kuszewski, J.; Nilges, M.; Pannu, N. S.; Read, R. J.; Rice, L. M.; Simonson, T.; Warren, G. L. *Acta Crystallogr. D Biol. Crystallogr.* **1998**, *54*, 905.
(42) van Aalten, D. M.; Bywater, R.; Findlay, J. B.; Hendlich, M.; Hooft, R. W.; Vriend, G. *J. Comput. Aided Mol. Des.* **1996**, *10*, 255.
(43) Pettersen, E. F.; Goddard, T. D.; Huang, C. C.; Couch, G. S.; Greenblatt, D. M.; Meng, E. C.; Ferrin, T. E. *J. Comput. Chem.* **2004**, *25*, 1605.
(44) DeLano, W. L. *Curr. Opin. Struct. Biol.* **2002**, *12*, 14.
(45) Nicholls, A.; Sharp, K. A.; Honig, B. *Proteins* **1991**, *11*, 281–296.
(46) Kamiya, T.; Teraji, T.; Hashimoto, M.; Nakaguchi, O.; Oku, T. *J. Am. Chem. Soc.* **1975**, *97*, 5020.
(47) Buynak, J. D.; Rao, A. S.; Nidamarthy, S. D. *Tetrahedron Lett.* **1998**, *39*, 4945.
(48) Efimovsky, O.; Rumpf, P. *Bull. Soc. Chim. Fr.* **1954**, 648.

of this oxide with phosphorus oxychloride produced chloromethylpyridine **28**,[49] which was subsequently converted to ylide **29**. Reaction of this ylide with the 6-oxopenicillinate **31** produced benzyhydryl 6*Z*-(α-pyridylmethylidene)penicillinate **32**, which was converted to the corresponding sulfone and deprotected to produce acid **34**. This acid was then converted to the unstable acyl azide, which was immediately thermolyzed in methanol to effect the Curtius rearrangement to the isocyanate, which was then trapped to produce carbamate **35**. Deprotection of the benzhydryl ester with TFA-anisole produced inhibitor **2**.

Last, the "east−west" dual-functionalized inhibitor **3** was synthesized as shown in SI Scheme 3. Thus, the functionalized 6-oxopenicillinate **12** (mixture with the corresponding cepham **13**) was treated with ylide **29** to produce a mixture of 6-alkylidenepenam (**37**) and 7-alkylidenecepham (**38**), as shown. As before, treatment with 1.5 equivalent of *m*CPBA effected the oxidation to the corresponding cepham sulfone and, primarily, the penam sulfoxide, which were separable. Further oxidation of the sulfoxide **39** to the sulfone **41**, followed by removal of the chloroacetate and the allyl ester protecting groups, produced hydroxyacid **43**. Treatment of this material with excess *p*-nitrophenyl chloroformate simultaneously converted the acid to the *p*-nitrophenyl ester and the alcohol to the *p*-nitrophenyl carbonate. Reaction with ammonia in dioxane produced the amidocarbamate intermediate **45**, which was subsequently deprotected to produce inhibitor **3** (compound **46**).

Microbiological Studies. In order to be an effective partner inhibitor for clinical use, the mechanism-based β-lactamase inactivator must effectively and rapidly penetrate the outer membrane of Gram-negative bacteria in sufficient concentrations to lower MICs into the susceptible range.[28] To establish a comparison, we employed the carbapenems that are used clinically (imipenem and meropenem) with the inhibitors at two different concentrations, 4 and 16 μg/mL. We also used tazobactam at the same concentrations as a comparator β-lactamase inhibitor. In order to ensure an appropriate contrast, we also expressed each of the different constructs in an isogenic host, the carbapenem-susceptible *A. baumannii* JC7/04 strain.[29] In contrast to laboratory strains of *Escherichia coli*, this model system ensures a more realistic appraisal of the efficacy of the compounds against the pathogen containing the $bla_{\text{OXA-24}}$.[50]

Against *A. baumannii* JC7/04 without OXA-24 expressed, the meropenem MICs are 1.0 μg/mL, well within the susceptible range.[31] In the genetic background where $bla_{\text{OXA-24}}$ in *A. baumannii* strain JC7/04 is expressed, high-level carbapenem resistance is observed (Table 2, meropenem and imipenem MIC = 32 μg/mL). When the inhibitor tazobactam, at 4 μg/mL, was combined with meropenem or imipenem, we did not detect a reduction in MICs (only slight, and no significant inhibition with imipenem). This is consistent with the clinical observation that β-lactam−tazobactam combinations are not effective against carbapenem-resistant isolates.[51,52] As each inhibitor possesses a β-lactam scaffold, we first tested each inhibitor without a partner antibiotic. Our results showed that compounds **1**−**5** do not possess any intrinsic antibiotic activity against *A. baumannii* JC7/04 with pAT-RA or pAT-RA with $bla_{\text{OXA-24}}$ (MIC ≥ 64 μg/mL). With respect to the inhibitory activity of compound **1** or **5** at 4 μg/mL combined with meropenem (Table 2a), we showed a noticeable reduction in MICs (32 to 4 μg/mL). Overall, MICs decreased more when the inhibitors were tested at a concentration of 16 μg/mL (Table 2b). This enhanced, "dose-dependent" effect was slightly more pronounced for meropenem than for imipenem. Overall, **1** combined with imipenem or meropenem reduced MICs better than any other combination.

Table 2. MIC Values of the Carbapenem-Susceptible *A. baumannii* Strain JC7/04 Transformants

	MIC (μg/mL)		
	pAT-RA[a]	pAT-RA/ OXA-24 (WT)	pAT-RA/OXA-24 (Y112A,M223A)
(a) Tazobactam and **1**−**5** Tested at 4 μg/mL			
meropenem	1	32	2
meropenem/tazobactam	0.5	32	2
meropenem/**1**	1	4	2
meropenem/**2**	1	16	2
meropenem/**3**	0.5	16	2
meropenem/**4**	0.5	16	1
meropenem/**5**	0.5	4	1
imipenem	1	32	4
imipenem/tazobactam	0.5	16	4
imipenem/**1**	0.5	4	4
imipenem/**2**	0.5	32	4
imipenem/**3**	0.5	8	4
imipenem/**4**	0.25	8	4
imipenem/**5**	0.5	8	4
(b) Tazobactam and **1**−**5** Tested at 16 μg/mL			
meropenem	1	32	2
meropenem/tazobactam	0.5	32	2
meropenem/**1**	1	1	0.5
meropenem/**2**	1	16	1
meropenem/**3**	0.5	4	0.5
meropenem/**4**	0.5	8	1
meropenem/**5**	0.5	4	1
imipenem	1	32	4
imipenem/tazobactam	0.25	16	2
imipenem/**1**	0.25	1	1
imipenem/**2**	0.25	16	4
imipenem/**3**	0.25	2	1
imipenem/**4**	0.25	4	2
imipenem/**5**	0.5	8	2

[a] Plasmid pAT-RA in *A. baumannii* without $bla_{\text{OXA-24}}$ gene. The MICs of tazobactam and **1**−**5** without meropenem or imipenem were >64 μg/mL.

We next measured the activity of the carbapenems against the variants possessing the Tyr112Ala,Met223Ala substitution (Table 2). As is shown by MICs, imipenem and meropenem resistance is reduced for the strain possessing the doubly substituted enzyme (that for WT is 32 μg/mL, and that for the doubly substituted enzyme is 2 or 4 μg/mL). This supports the observation that the two residues, Tyr112Ala and Met223Ala, also play a critical role in resistance to carbapenems.[29] The MICs were slightly reduced when each of the inhibitors was combined with meropenem or imipenenem against the doubly substituted enzyme (especially at 16 μg/mL).

Kinetic Parameters. In the steady-state experiments summarized in SI Table 1, the OXA-24 β-lactamase and variants studied were purified to greater than 95% homogeneity. The WT enzyme, OXA-24 β-lactamase, hydrolyzed NCF with $k_{\text{cat}}/K_{\text{m}} = 19.2 \pm 2.6\ \mu\text{M}^{-1}\,\text{s}^{-1}$ (SI Table 1). This robust activity was similar to the hydrolysis of NCF by OXA-1[28,33] and ranks with the high catalytic efficiency demonstrated by class A β-lactamases toward penicillins and certain class C enzymes

(49) Ash, M. L.; Pews, R. G. *J. Heterocycl. Chem.* **1981**, *18*, 939.
(50) Sato, K.; Nakae, T. *J. Antimicrob. Chemother.* **1991**, *28*, 35.
(51) Hujer, K. M.; Hujer, A. M.; Hulten, E. A.; Bajaksouzian, S.; Adams, J. M.; Donskey, C. J.; Ecker, D. J.; Massire, C.; Eshoo, M. W.; Sampath, R.; Thomson, J. M.; Rather, P. N.; Craft, D. W.; Fishbain, J. T.; Ewell, A. J.; Jacobs, M. R.; Paterson, D. L.; Bonomo, R. A. *Antimicrob. Agents Chemother.* **2006**, *50*, 4114.
(52) Perez, F.; Hujer, A. M.; Hujer, K. M.; Decker, B. K.; Rather, P. N.; Bonomo, R. A. *Antimicrob. Agents Chemother.* **2007**, *51*, 3471.

Table 3. Kinetic Parameters of Inhibition

compd		K_i (μM)[a]	k_{inact} (s^{-1})	k_{inact}/K_i ($\mu M^{-1}s^{-1}$)
1	OXA-24 WT	0.70 ± 0.05	0.15 ± 0.01	0.21 ± 0.02
2	OXA-24 WT	2.3 ± 0.3	0.05 ± 0.01	0.022 ± 0.005
3	OXA-24 WT	1.6 ± 0.3	0.25 ± 0.02	0.16 ± 0.02
4	OXA-24 WT	0.50 ± 0.08	0.09 ± 0.01	0.18 ± 0.03
5	OXA-24 WT	4.1 ± 0.6	0.08 ± 0.01	0.020 ± 0.003

[a] Tazobactam K_i was determed by Drawz et al. to be 271 ± 37 μM.

toward cephalosporins.[53−55] Categorically, OXA enzymes are regarded as carboxy-penicillinases and amino-penicillinases.[16] Since OXA-24 is characterized as a carbapenemase, we next measured the catalysis of imipenem as a reference carbapenem. In keeping with susceptibility testing (MIC = 32 μg/mL), we observed that the hydrolysis of imipenem was measurable [$k_{cat}/K_m = 1.7 \pm 0.2$ μM^{-1} s^{-1} (SI Table 1)]. Interestingly, the k_{cat} of imipenem was much lower when compared to the k_{cat} of NCF. This finding is consistent with the observation made by Queenan and Bush that OXA carbapenemases have a high apparent affinity for carbapenems but a low turnover.[10]

The singly (OXA-24 Tyr112Ala) and doubly (OXA-24 Tyr112Ala,Met223Ala) substituted enzymes demonstrated less robust activity (14% activity of the WT vs NCF; 14−24% of the WT vs imipenem). Each of the variants showed higher K_m values for NCF (OXA-24 Tyr112Ala, $K_m = 238$ μM; OXA-24 Tyr112Ala,Met 223Ala, $K_m = 143$ μM).

In order to enrich our understanding of the mechanism of inhibition, two approaches were used to assess the efficacy of the inhibitors against OXA-24 and the OXA-24 variants. As discussed previously, the appropriate biochemical correlates that translate into effective β-lactamase inhibition in a clinical setting are complex and multifactorial (cell penetration, pharmacodynamics, pharmacokinetics, etc.).[17] These considerations are fundamental to the assessment of each inhibitor, as OXA-24 is resistant to the commercially available inhibitors and is expressed in the *Acinetobacter* spp. background.

To begin, we first measured IC_{50} values at 10 min using CENTA, as this parameter informs us of the relative effectiveness of an inhibitor. The IC_{50} values for all four inhibitors against the OXA-24 β-lactamase ranged from 127 ± 42 (**1**) to 237 ± 7 nM (**5**) (SI Table 2a). We also noted a slight increase in the IC_{50} values with respect to the four inhibitors when tested against the singly and doubly substituted enzyme, but this increase was not enough to confer inhibitor resistance (≤ 1 μM).

In a similar manner, we determined IC_{50} values using NCF. As the chemical properties and affinities of CENTA are different than NCF (both are indicator substrates), this served as a confirmation of the affinities of the compounds for OXA-24 and variants. As is evident from the data in SI Table 2b, the inhibitors demonstrated a 10-fold greater affinity (lower IC_{50} values) with NCF than with CENTA.

To more precisely identify the correlates of inactivation and inhibition, we next determined the K_i and the inactivation efficiency (k_{inact}/K_i) of each inhibitor (Table 3 and SI Table 3). We examined the activity of each of these inhibitors against the WT enzyme and the two variants.

Notably, **4** and **1** showed the lowest K_i for WT, followed by **3**, **2**, and **5**. Compound **1** possessed the highest inactivation efficiency ($k_{inact}/K_i = 0.21 \pm 0.02$ μM^{-1} s^{-1}) (Table 3). With regard to the two variant OXA β-lactamases, we see for the five inhibitors an overall lowering of inactivation efficiencies (k_{inact}/K_i) due to decreases in k_{inact} and increases in K_i (SI Table 3).

We note that there is a difference between the kinetic parameters obtained measuring IC_{50} and K_i measurements vs microbiological values. We reconcile this difference by positing that the ability and rate of each of the inhibitors to penetrate across the outer membrane of this strain of *A. baumannii* may be different.[50] Factors such as permeability coefficients, diffusion rates, and the presence or absence of specific porins may be important here and merit further studies.[56,57] The design of **1** attempts to enhance transport across the cell membrane.[26]

ESI-MS. To establish the nature of the inactivation products, ESI-MS was performed with a Q-Star quadrupole time-of-flight mass spectrometer equipped with a nanospray source. We inactivated OXA-24 β-lactamase with each of the inhibitors. The incubation (inactivation) time was 15 min (900 s). The deconvoluted spectra are presented in SI Figure 1, and our results are summarized in SI Table 4. The ESI-MS measurements ($29\,071 \pm 3$ amu) were in agreement with the theoretical mass of the OXA-24 β-lactamase, which is 29 073 (this includes the five additional amino acids at the N-terminus as a result of the cloning procedure). The preparative method did not permit us to identify a mass increase consistent with the addition of a CO_2 group (carboxylation at Lys84) to the β-lactamase.

Covalent attachment of each inhibitor to the OXA-24 β-lactamase and variant enzymes was demonstrated in each of the spectra. During the time period studied, we did not find evidence of the fragmentation of the inhibitors, as was seen in the inactivation of TEM-1, CMY-2, SHV-1, the Arg244Ser variant of SHV-1, and the Ser130Gly variant of SHV-1 with tazobactam and clavulanate.[58−64] These observations were further rationalized after examination of the mechanisms of inactivation.

Crystallography. We next solved the crystal structures of OXA-24 complexed with different penicillin sulfone-based inhibitors (**1**, **2**, **3**, and **5**). This offered us an unprecedented opportunity to compare the inactivation mechanisms of different inhibitors of the same chemical series with different K_i values. Structures were solved by Fourier synthesis employing the coordinates of the native enzyme. After rigid-body refinement and model fitting, the position of the inhibitors was clearly defined in the active site covalently attached to Ser81. The overall fold of the complexes was similar to the native OXA-24 structure.[29]

(53) Bauvois, C.; Ibuka, A. S.; Celso, A.; Alba, J.; Ishii, Y.; Frère, J. M.; Galleni, M. *Antimicrob. Agents Chemother.* **2005**, *49*, 4240.
(54) Bulychev, A.; Mobashery, S. *Antimicrob. Agents Chemother.* **1999**, *43*, 1743.
(55) Jacoby, G. A. *Clin. Microbiol. Rev.* **2009**, *22*, 161.
(56) Lakaye, B.; Dubus, A.; Joris, B.; Frère, J. M. *Antimicrob. Agents Chemother.* **2002**, *46*, 2901.
(57) Lakaye, B.; Dubus, A.; Lepage, S.; Groslambert, S.; Frère, J. M. *Mol. Microbiol.* **1999**, *31*, 89.
(58) Bonomo, R. A.; Liu, J.; Chen, Y.; Ng, L.; Hujer, A. M.; Anderson, V. E. *Biochim. Biophys. Acta* **2001**, *1547*, 196.
(59) Brown, R. P.; Aplin, R. T.; Schofield, C. J. *Biochemistry* **1996**, *35*, 12421.
(60) Brown, R. P.; Aplin, R. T.; Schofield, C. J.; Frydrych, C. H. *J. Antibiot.* **1997**, *50*, 184.
(61) Helfand, M. S.; Bethel, C. R.; Hujer, A. M.; Hujer, K. M.; Anderson, V. E.; Bonomo, R. A. *J. Biol. Chem.* **2003**, *278*, 52724.
(62) Sulton, D.; Pagan-Rodriguez, D.; Zhou, X.; Liu, Y.; Hujer, A. M.; Bethel, C. R.; Helfand, M. S.; Thomson, J. M.; Anderson, V. E.; Buynak, J. D.; Ng, L. M.; Bonomo, R. A. *J. Biol. Chem.* **2005**, *280*, 35528.
(63) Thomson, J. M.; Distler, A. M.; Prati, F.; Bonomo, R. A. *J. Biol. Chem.* **2006**, *281*, 26734.
(64) Yang, Y.; Janota, K.; Tabei, K.; Huang, N.; Siegel, M. M.; Lin, Y. I.; Rasmussen, B. A.; Shlaes, D. M. *J. Biol. Chem.* **2000**, *275*, 26674.

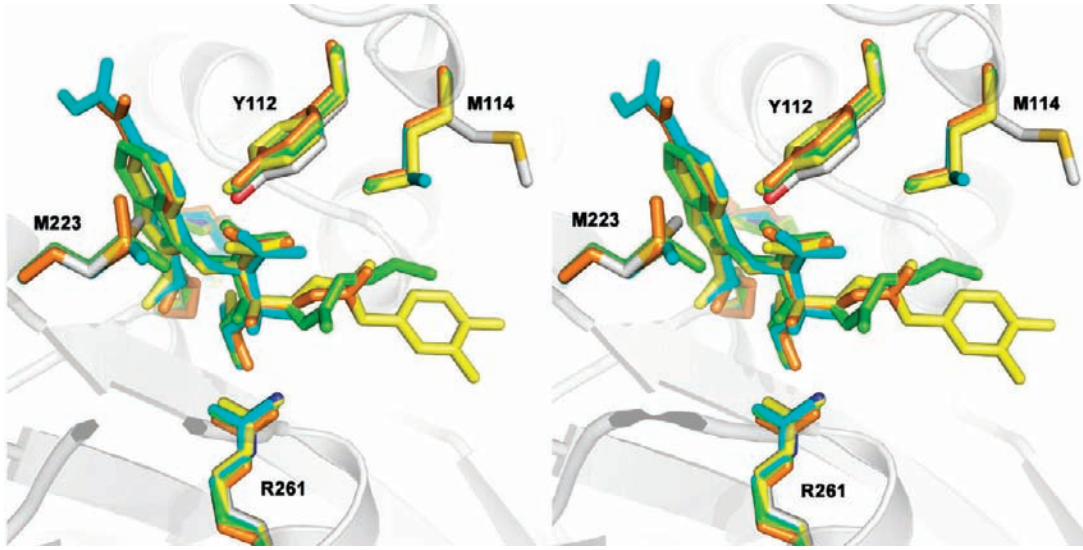

Figure 2. Stereoview of the superposition at the active binding site of native OXA-24/40 (gray) and complexes with **1** (yellow), **2** (cyan), **3** (orange), and **5** (green). The secondary structure of the enzyme is in gray. For clarity, only side-chain residues implicated in binding are represented. In the active site, major changes are not observed upon inhibitor binding, but several modifications are seen in active-site residues directly involved in inhibitor accommodation.

When complexed to inhibitors, the conformations of the active site are very similar to that observed in the native enzyme, although several changes can be appreciated. The side chains of Tyr112 and Arg261 reorient slightly (~0.6 Å) to accommodate the sulfinic and carboxylate groups of the inhibitors (Figure 2).

The initial omit electron density maps strongly indicated the formation of an acyl-enzyme intermediate containing a bicyclic aromatic ring system composed of two fused aromatic rings, a five-membered ring fused to a six-membered pyridine ring (Figure 3). The electron density and structures of **3** soaked at different time points (**3** and **3b**, Figure 3A,B,C) indicate that the bicyclic inhibitor intermediate is quite stable during the 5−15 min time period. This aromatic indolizine system points toward the solvent region and sterically blocks the entry to the catalytic cleft on the left side of the tunnel-like cavity. Contrary to what was found in SHV-1 and SHV-2 class A β-lactamases complexed with **1**,[26] the carbonyl oxygen of the intermediates of **2**, **3**, and **5** is located *in* the oxyanion hole, forming hydrogen bonds to the backbone amide of Trp121 (2.9 Å), in a similar manner to that found in the structure of the class C GC1 β-lactamase with the reaction product of the sulfone DVR-II-41S.[65] The side chains of the ring-derived system extending from C2 in the three inhibitors also show other significant contacts with the enzyme.

We stress that the network of interactions which clearly contributes to the stability of the intermediate is strictly conserved for the inhibitors **2**, **3**, and **5** (Figure 4). The sulfinate anion is in close proximity to the guanidinium group of Arg261, establishing strong salt-bridge interactions (2.67 and 3.02 Å). Besides this electrostatic interaction, OXA-24 still also makes strong hydrogen bonds to the hydroxyl groups of Ser128 (3.04 Å) and Ser219 (2.52 Å), two highly conserved residues at the active site. The orientation adopted by the sulfinate anion emulates the positioning of the carboxylate moiety of the antibiotic, as was reported in other acyl-enzyme complexes with meropenem.[66,67] As a consequence of this orientation, the carboxylate group folds back over the tunnel, establishing a strong hydrogen bond with the hydroxyl group of Tyr112 (2.8 Å), one of the key residues that form the tunnel-like entrance to the active site in OXA-24 (Supporting Information Figure 2A,B).[29] Apart from this common interaction network, the remaining contacts between the intermediate and the enzyme vary depending on the chemical nature of the inhibitor. Thus, the effect of the substituents at the pyridylmethylidene moiety in the stabilization of the acyl-enzyme intermediate can only be described for compounds **2** and **3**. Whereas the carbamoyl group of compound **3** is in close contact with the hydroxyl group of Thr111 (3.06 Å), the methoxycarbamoyl substituent on compound **2** has not revealed additional interactions with the enzyme (Figure 4A,B).

On the other hand, the more complex tailored substituents at position C2 of the penicillin sulfone ring do not show favorable interactions to provide an additional stabilization of the intermediate, with exception of the 3,4-(dihydroxyphenyl)acetate of **1**. Unfortunately, the electron density maps for the **1** inhibitor do not show a clearly defined position for the catechol moiety of the inhibitor, and also the population of the central core is not full, perhaps indicating disorder or partial site occupancy (data not shown). However, it can be said that the bulky group at C2 runs almost parallel to the right side of the active site by stacking the catechol moiety with various residues on the hydrophobic surface of the enzyme (SI Figure 2A). Stacking of **1**'s catechol moiety has also been observed in its complex with SHV-1.[26]

The combined results imply that the stable acyl-enzyme complexes from the 6-alkylidene-2′-substituted penicillin sulfone inhibitors are formed by a sequence of events in which initial nucleophilic attack of Ser81 O^{γ} on the carbonyl of the penicillin ring releases the β-lactam nitrogen lone pair,

(65) Crichlow, G. V.; Nukaga, M.; Doppalapudi, V. R.; Buynak, J. D.; Knox, J. R. *Biochemistry* **2001**, *40*, 6233.

(66) Nukaga, M.; Bethel, C. R.; Thomson, J. M.; Hujer, A. M.; Distler, A.; Anderson, V. E.; Knox, J. R.; Bonomo, R. A. *J. Am. Chem. Soc.* **2008**, *130*, 12656.

(67) Pernot, L.; Frenois, F.; Rybkine, T.; L'Hermite, G.; Petrella, S.; Delettre, J.; Jarlier, V.; Collatz, E.; Sougakoff, W. *J. Mol. Biol.* **2001**, *310*, 859.

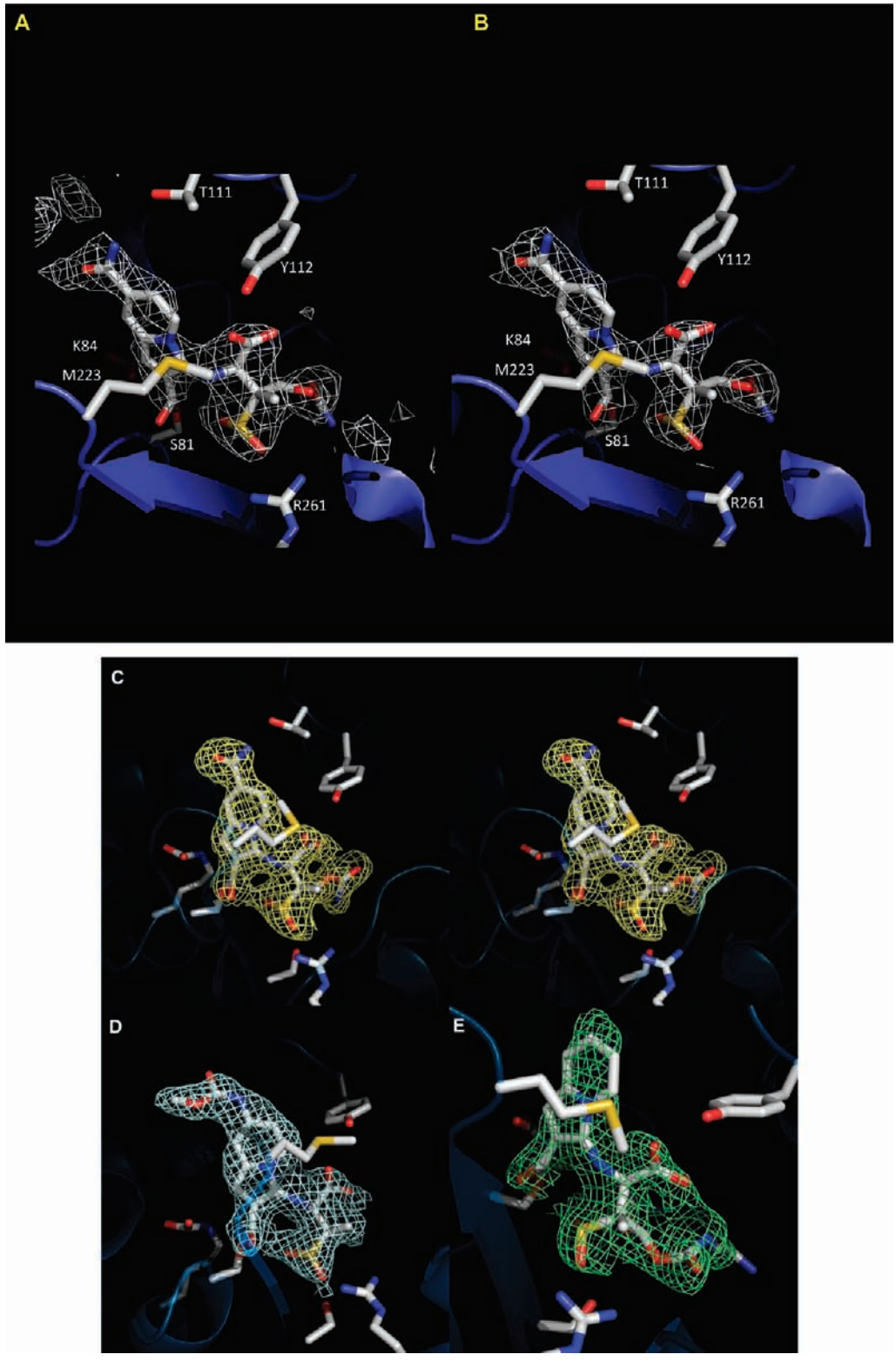

Figure 3. Binding mode of the substituted penicillin sulfone inhibitors in the active site of OXA-24 b-lactamase. (A) Initial $F_o - F_c$ omit maps for **3b** contoured at 3.0σ. Final $2F_o - F_c$ electron density maps for (B) **3b** at 2.6 Å resolution, (C) **3** at 2.1 Å resolution in stereoview, (D) **2** at 2.0 Å resolution, and (E) **5** at 2.0 Å resolution; contour levels are at 1.0σ. The maps show a clear density for an intermediate containing an indolizine moiety as a result of the formation of a five-membered ring fused to the pyridine ring extending from the 6-alkylidene substituted penicillin sulfone inhibitors.

thus enabling the opening of the neighboring sulfone ring. Another rearrangement provided by the pyridyl nitrogen bonded to the former C5 of the resultant imine leads to the formation of the crystallographically observed indolizine system.

In each of the inhibitor complexes, the π system of the acyl-enzyme carbonyl is orthogonal to the π system of the bicylic indolizine. Thus, it is clear that the hydrolytic stability of the covalent ester linkage is not due to a resonance interaction with the nitrogens (i.e., β-aminoacrylate or "enamine") or to interac-

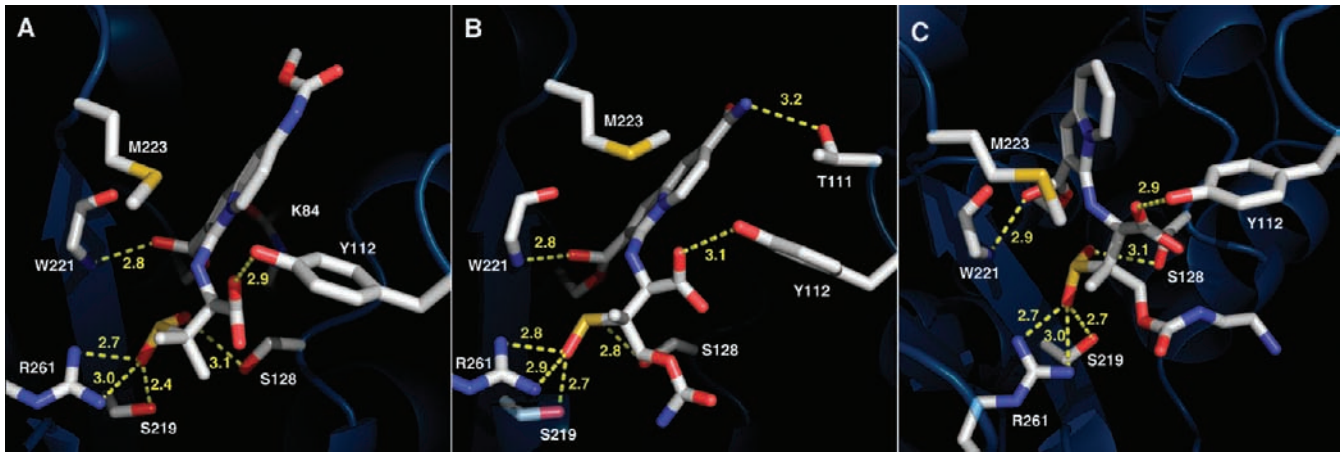

Figure 4. Active site and inhibitor interactions. Detailed interactions in the active site of OXA-24 with (A) **2**, (B) **3**, and (C) **5**. The indolizine aromatic ring is visibly anchored into the tunnel-like cavity of the binding site through its conjugated acyl group covalently attached to the catalytic serine residue Ser81. The secondary structure of the enzyme is in blue. The side chains of the ligand-binding residues and inhibitors are represented in ball-and-stick mode. Selected interacting residues are labeled, and hydrogen bonds are indicated by dotted lines.

tion of the ester carbonyl with the aromatic system. What is stabilizing these acyl-enzymes toward hydrolysis? Notably absent in all structures is a hydrolytic water molecule proximal to both the carboxylated lysine and the acyl-enzyme carbonyl carbon. It has been observed that, unlike for the corresponding class A β-lactamases, a crystallographically observable hydrolytic water molecule is not seen in the class D apoenzymes, and it is assumed that such a water must diffuse into the site after formation of the acyl-enzyme.[68] However, in the case of these inhibitors, the active site is occupied by the conformationally rigid bicyclic indolizine moiety, prospectively preventing the entry of extraneous water, and thus stabilizing the acyl-enzyme (SI Figure 2B,C).

Based upon previous insights proposed by Golemi et al., a likely mechanism for the inactivation of OXA-24 β-lactamase is shown in Scheme 2.[69] An interesting feature of the mechanism is that, relative to the normal hydrolytic process (Scheme 2, panel B), the inhibitor provides the enzyme with one extra proton, which is lost from C5 of the inhibitor in order to achieve aromaticity (Y $\rightarrow$ Z, Scheme 2, panel A). This would then leave the carboxylated lysine as its conjugate acid and thus unable to activate water for hydrolysis of the acyl-enzyme. Note that, in the case of the penam substrate (bottom), the carbamic acid can be deprotonated by the proximal amine (previously N4 of the penam), while, in the case of the inhibitor, N4 is rendered significantly less basic due to its conjugation with the indolizine and interaction with the acyl-enzyme carbonyl.

This mechanism also illustrates the ability of the OXA-24 carboxylated lysine to repetitively cycle between its conjugate acid and base forms and acyl and apo states, thus differentiating these catalytic class D β-lactamases from the highly homologous sensor domain of the BlaR1 protein from *Staphylococcus aureus*. In the case of BlaR1, the formation of the acyl-enzyme (and consequent formation of the carboxylysine conjugate acid) results in decarboxylation, thus removing the proximal base and fixing the sensor in the acylated ("on") state, as shown in Scheme 3.[70] Through an unknown mechanism, this acylated form results in a conformational change of the transmembrane domain and relays a signal to the cytoplasm, leading to the proteolytic degradation of a repressor protein, thus de-repressing the *blaZ* gene and leading to production of more β-lactamase. In contrast to the catalytic action of the class D β-lactamases, the BlaR1 protein is irreversibly acylated by penicillins, presumably as a consequence of the lysine decarboxylation which occurs upon acylation (and formation of the conjugate acid of the carbamic acid).[71,72]

Ab initio quantum chemical studies have shown that the activation energy for the decarboxylation of carbamic acids is lowered by 44 kcal mol^{-1} by the presence of one molecule of water in the transition state, as shown in Scheme 3.[73] As shown in Figure 5, comparison of the respective active sites reveals a key structural difference between the BlaR1 sensor and class D β-lactamases: the presence of a highly conserved hydrophobic residue at the β-lactamase position 130 (OXA-24 numbering, Val or Ile, corresponds to position 120 using DBL consensus numbering), in contrast to a hydrophilic residue (Asn in case of *S. aureus*, or Thr in the case of *Bacillus licheniformis*[74]) at the corresponding BlaR1 position. Additionally, as shown, two proximal water molecules were found in the 1XA1 BlaR1 apoenzyme, prospectively providing the precise water molecule involved in this decarboxylation.[75]

Conclusions

OXA carbapenemases are becoming one of the most clinically important resistance determinants found in *A. baumannii*.[16] Most clinical isolates of *A. baumannii* are resistant to narrow-spectrum and extended-spectrum cephalosporins due to the expression of the chromosomally encoded AmpC β-lactamase, called

(68) Sun, T.; Nukaga, M.; Mayama, K.; Braswell, E. H.; Knox, J. R. *Protein Sci.* **2003**, *12*, 82.
(69) Golemi, D.; Maveyraud, L.; Vakulenko, S.; Samama, J. P.; Mobashery, S. *Proc. Natl. Acad. Sci. U.S.A.* **2001**, *98*, 14280.
(70) Cha, J.; Mobashery, S. *J. Am. Chem. Soc.* **2007**, *129*, 3834.
(71) Birck, C.; Cha, J. Y.; Cross, J.; Schulze-Briese, C.; Meroueh, S. O.; Schlegel, H. B.; Mobashery, S.; Samama, J. P. *J. Am. Chem. Soc.* **2004**, *126*, 13945.
(72) Thumanu, K.; Cha, J.; Fisher, J. F.; Perrins, R.; Mobashery, S.; Wharton, C. *Proc. Natl. Acad. Sci. U.S.A.* **2006**, *103*, 10630.
(73) Ruelle, P. K.; Ho Nam-Tran., U. W. *Theochem—J. Mol. Struct.* **1985**, *25*, 41.
(74) Kerff, F.; Charlier, P.; Colombo, M. L.; Sauvage, E.; Brans, A.; Frere, J. M.; Joris, B.; Fonze, E. *Biochemistry* **2003**, *42*, 12835.
(75) Wilke, M. S.; Hills, T. L.; Zhang, H. Z.; Chambers, H. F.; Strynadka, N. C. *J. Biol. Chem.* **2004**, *279*, 47278.

Scheme 2. Proposed Mechanism of OXA-24 β-Lactamase Inhibition by **5**

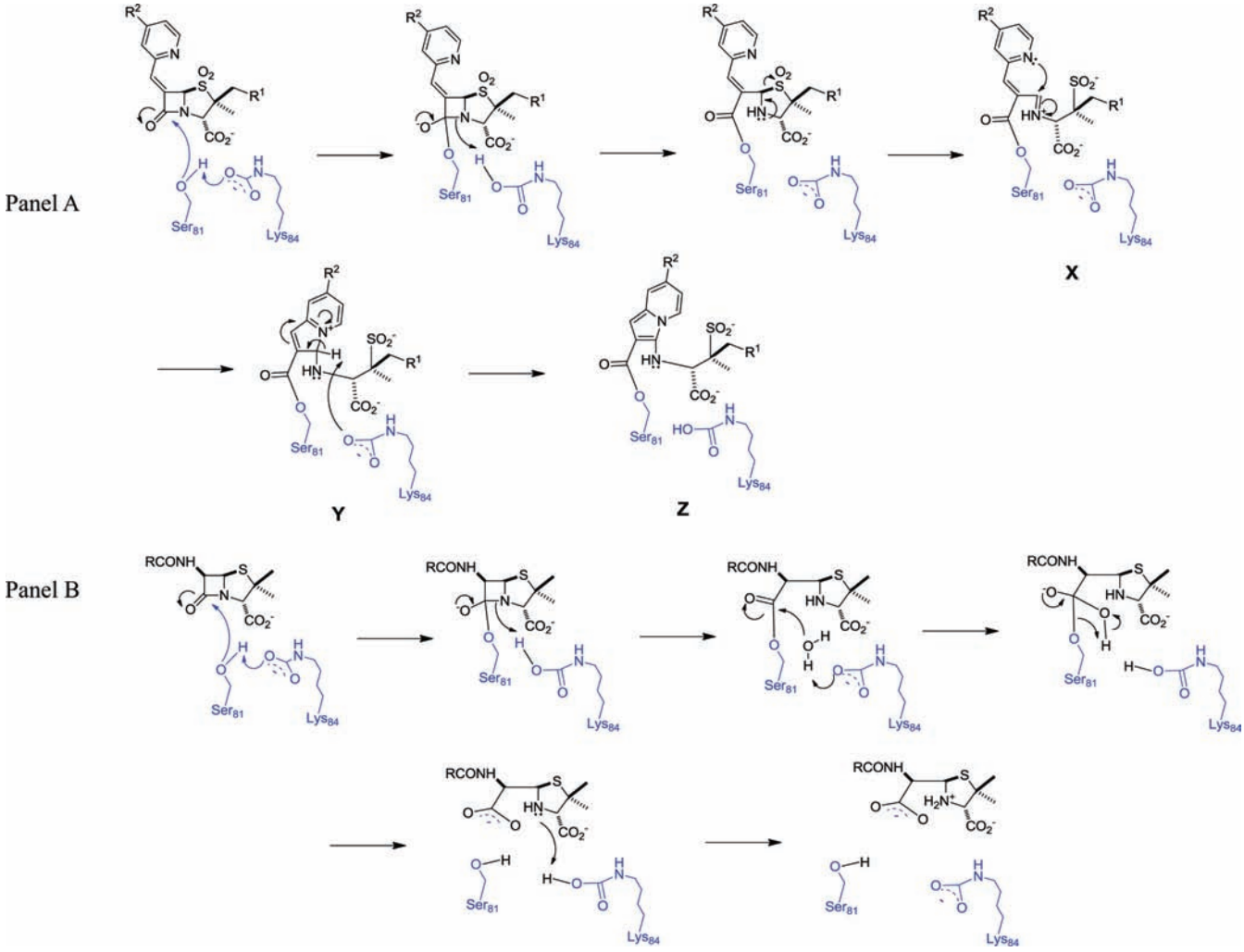

Scheme 3. Proposed Mechanism for the Formation of the BlaR1 Acyl-Enzyme

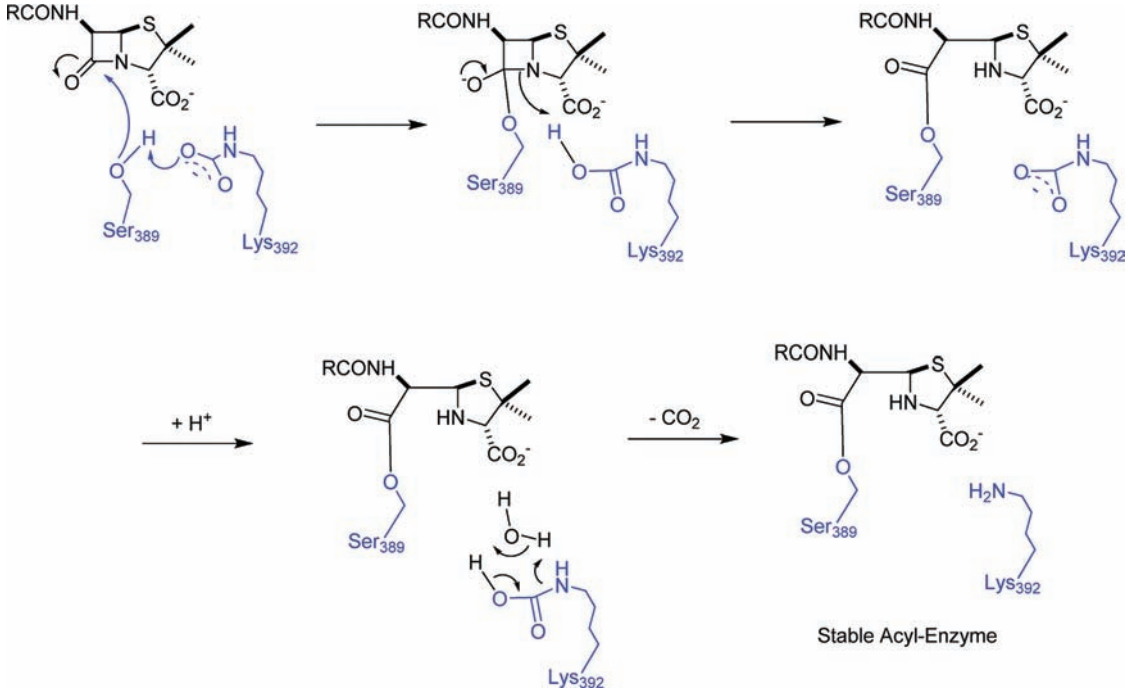

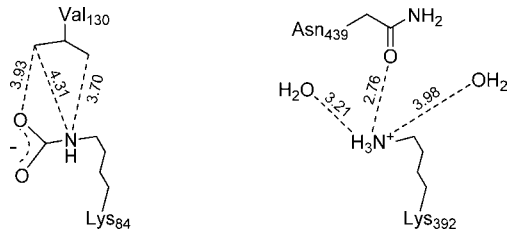

Figure 5. Comparison of the active-site carboxylysine environment of OXA-24 (left, 3G4P) with BlaR1 (right, 1XA1).

Acinetobacter-Derived Cephalosporinase (ADC).[51,76] An examination of the current clinical experience shows that OXA-23, -24, -51, -58, -69, and -72 seem to be very prevalent among outbreaks of carbapenem-resistant *A. baumannii*.[16] At present, there are only two carbapenem-hydrolyzing class D enzyme (OXA-48 and OXA-24) crystal structures available for study.

As shown by Santillana et al., the crystal structure of OXA-24 β-lactamase revealed several unique features.[29] In contrast, the structure of OXA-48 at 1.9 Å was overall similar to the crystal structure of OXA-10, a class D β-lactamase that does not hydrolyze imipenem.[77] The present work captures for the first time the crystal structure of novel 6-alkylidene-2′-substituted penicillanic acid sulfones as active-site inhibitors of OXA-24. This work significantly extends the previous studies with **1** in class A enzymes to a class of β-lactamases that has escaped inhibition by commercial inhibitors.[26]

Five important insights are obtained from this analysis. First, with these inhibitors, we see the formation of a stable, unfragmented adduct with the carbonyl oxygen positioned deep in the oxyanion hole. Normally, one would expect that this conformation would facilitate hydrolysis as opposed to inhibition. Yet, the unique reaction chemistry followed by these C6-substituted compounds involves formation of a bicyclic aromatic ring that may impede approach of an attacking water molecule. This adds an additional feature, enhancing these molecules (a theme reminiscent of DVR-II-41S, see ref 65). This is in stark contrast to what was seen with SHV-1 β-lactamase[26] because of the positioning of the intermediate carbonyl oxygen.

Second, the negatively charged sulfinate group on each of these compounds is positioned to interact via a stabilizing salt bridge with the residue Arg261. The strong H bonds to Ser128 and 219 also add to this stability.

Third, the carboxylate of the inhibitor, folding over to make an H bond to Tyr112, further enhances the stability of the complex.

Fourth, a new and previously unappreciated feature of these penicillin sulfones may be their capability to provide an extra proton to the active site, thus generating the conjugate acid of the carboxylysine and interrupting the catalytic process.

Finally, a comparison of the environment surrounding the carboxylysine of the class D β-lactamases with that of the highly homologous BlaR1 sensor protein reveals that the class D β-lactamases have a significantly more hydrophobic environment. The more hydrophilic environment of the carboxylysine of BlaR1 may explain its rapid decarboxylation, since it is known that the transition state for decarboxylation of carbamic acids is significantly lowered by incorporating one molecule of water in the process. Relative to ongoing catalysis, this decarboxylation also requires at least one additional proton, thus potentially providing a mechanism to induce the large conformational shift needed for intracellular signaling.

Taken together, our findings point to an effective strategy to inhibit not only this OXA carbapenemase but also other serine-based enzymes that inactivate β-lactam antibiotics, and they provide several intriguing hypotheses to be explored with respect to the highly homologous BlaR1 sensor protein. A comparative analysis against other OXA carbapenem-hydrolyzing and extended-spectrum OXA β-lactamases enzymes is warranted, as the pathways to evolution of these enzymes are different.[77] The quest to find inhibitors active against a wide range of carbapenem hydrolyzing enzymes will remain a persistent challenge as the diversity in class D grows.

Acknowledgment. J.D.B. was supported by the Robert A. Welch Foundation, Grant N-0871. F.v.d.A. is supported by National Institutes of Health (R01 AI062968). The Veterans Affairs Merit Review Program, GRECC, and the National Institutes of Health (RO1 AI063517-01) supported R.A.B. We thank the staff of the ESRF (France) and the National Synchrotron Light Source (Brookhaven National Laboratory) for technical assistance. A.R. was funded by BFU2008-02595 and CSD2009-00088 from the Ministerio de Educación y Ciencia (Spain) and the Regional Government of Madrid (PBio-0214-2006). G.B. was funded by FIS (PI061368, PI081613, PS09/00687) from the Instituto de Salud Carlos III (Spain).

Supporting Information Available: SI Tables 1−4, listing kinetic parameters, IC_{50} values, and ESI-MS data; SI Schemes 1−3 showing the syntheses of **2**−**5**; and SI Figures 1 and 2 showing mass spectra, detail of the region at the lower border of the active binding cleft of the **1** complex, and close-up views of the surface potential at the active binding site of OXA-24 in complex with **5**. This material is available free of charge via the Internet at http://pubs.acs.org.

JA104092Z

(76) Hujer, K. M.; Hamza, N. S.; Hujer, A. M.; Perez, F.; Helfand, M. S.; Bethel, C. R.; Thomson, J. M.; Anderson, V. E.; Barlow, M.; Rice, L. B.; Tenover, F. C.; Bonomo, R. A. *Antimicrob. Agents Chemother.* **2005**, *49*, 2941.

(77) Docquier, J. D.; Calderone, V.; De Luca, F.; Benvenuti, M.; Giuliani, F.; Bellucci, L.; Tafi, A.; Nordmann, P.; Botta, M.; Rossolini, G. M.; Mangani, S. *Chem. Biol.* **2009**, *16*, 540.